49th AIAA Aerospace Sciences Meeting including the New Horizons Forum and Aerospace Exposition
4 - 7 January 2011, Orlando, Florida
AIAA 2011-908

A Computational Diagnostic Tool for Understanding Plasma Sterilization

Navya Mastanaiah[1] & Chin Cheng Wang[2]
Applied Physics Research Group (APRG)
Department of Mechanical & Aerospace Engineering
University of Florida, Gainesville, FL 32611-6300

Judith A. Johnson[3]
Department of Pathology, Immunology & Laboratory Medicine
College of Medicine, and Emerging Pathogens Institute
University of Florida, Gainesville, FL 32610-0009

Subrata Roy[4]
Applied Physics Research Group (APRG)
Department of Mechanical & Aerospace Engineering
University of Florida, Gainesville, FL 32611-6300

Plasma sterilization is fast evolving into a sought after sterilization method in industries such as medicine, biology, food and healthcare. Atmospheric, non-thermal dielectric barrier discharge (DBD) plasma poses certain advantages in terms of sterilization: it is fast, non-toxic and versatile. While abundant research deals with several different plasma types (inductive, capacitive, microwave) and their application to different kinds of bacteria and spores, the need for a deeper intuitive understanding of the fundamental plasma processes is being realized. We propose using the rate of ionization, determined by computational simulations, as a marker to obtain the killing rate in plasma sterilization processes.

I. Introduction

Before we dive into the 'how' and 'what' of this paper, a few words on plasma, specifically Dielectric Barrier Discharge (DBD) plasma, sterilization and the application of DBD plasma to sterilization are warranted.

Plasma, also known as the fourth state of matter, is loosely described as an ionized gas consisting of neutrals, ions, electrons and UV photons. The definition of ionized gas has to be regarded with a little more care here, as even a jet exhaust is weakly ionized gas. The difference between them is that the collisions between radicals and electrons in a jet exhaust are controlled more by hydrodynamic forces than electromagnetic forces. Hence parameters such as Debye length (λ_D), plasma frequency (ω) and the Debye sphere (N_D) come into play[1].

A discussion on plasma and its properties is not complete without referring to the V-I characteristic for a plasma discharge [2], [16]. This characteristic shows that the plasma regime is divided into different types of discharges: dark discharge, glow discharge and arc. Each regime is characterized by certain properties common to all plasmas formed in that regime. For instance, consider the Townsend discharge, which is created by an electron avalanche and is a self-sustained dark discharge. As the transition to a sub-normal and normal glow discharge [1]

---

[1] Graduate Student, Mechanical & Aerospace Engineering, University of Florida, student member, AIAA
[2] Post doctoral associate, Mechanical & Aerospace Engineering, University of Florida, student member, AIAA
[3] Professor & Director of CORE Laboratories, College of Medicine, University of Florida
[4] Associate Professor, Mechanical & Aerospace Engineering Department, University of Florida, Associate Fellow, AIAA

occurs, it is seen that voltage decreases accompanied by an increase in discharge current. An abnormal glow discharge occurs as current increases further, finally transitioning irreversibly into the arc.

Now that the definition and basic properties of a plasma have been sufficiently reviewed, the next topic to consider would be the Dielectric Barrier Discharge (DBD) plasma, more specifically, the Atmospheric Pressure DBD plasma (APDBD). DBDs have been known as early as 1857, when Werner Von Siemens [3] first reported experiments wherein O_2 or air, flowing in a narrow gap between two coaxial annular electrodes was subjected to an alternating electric field. DBDs were used in ozone generation for a long time. More recently, they have also been applied in plasma chemical vapor deposition, pollution control and LCD display panels. The DBD discharge is produced when an alternating voltage is applied between two electrodes, with a dielectric in between them or at least one of the electrodes covered by a dielectric. The dielectric also acts as ballast: it imposes an upper limit on the current density in the gap. The DBD discharge is extinguished when the electron current is terminated or the electric field collapses. Typically DBDs are operated at a voltage of 1-100 kV and frequencies of 50 Hz-1 MHz. They are characterized by the presence of streamer like filaments and micro-discharges.

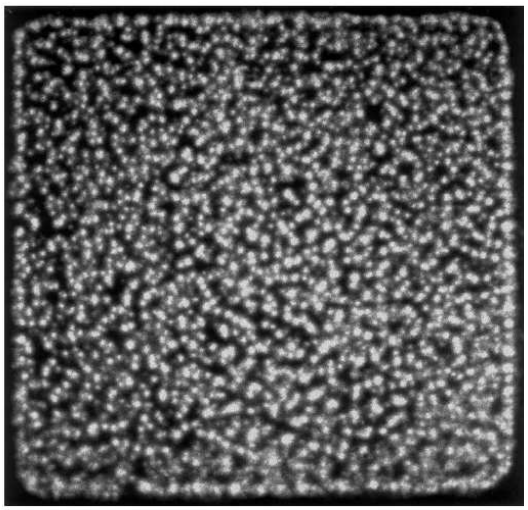

Fig.1.End on view of micro-discharges in atmospheric pressure air [3]

APDBD can be used for sterilization. Sterilization is defined as any process that destroys all micro-organisms, with bacterial endospores being the most difficult to kill. Disinfection is a lower target ndicatoffing several orders of magnitude reduction in microbial concentration, while sterilization indicates complete killing and is generally tested with a challenge of . Hence while alcohol based sanitizers and household cleaning products can work very well for low level disinfection, high level disinfection and sterilization suitable for use on medical instruments require a different arsenal of tools. This includes conventional methods of sterilization such as autoclaving and ethylene oxide fumigation as well as more recent methods such as UV irradiation. The conventional methods of sterilization have been well discussed in a previous paper by the authors [16]. In summary, these methods are proven effective methods, but have their own disadvantages such as long sterilization times, toxicity and handling difficulties. Atmospheric pressure non-thermal plasma sterilization trumps these methods owing to its advantages of short sterilization times, little toxicity and versatility.

So while there is abundant literature on DBD plasma and its application in various experimental scenarios using various biological indicators [4]-[8], there is not enough literature that concentrates more on understanding the fundamental processes involved in plasma sterilization. Fridman[9], in his book writes a fascinating chapter, analyzing plasma processes. Different chemical reactions that can take place in plasma, between the various chemical radicals are reviewed. Other tools such as spectroscopy, gel electrophoresis, fluorescent arrays have also been used to further quantify the plasma processes and assign a definite kinetic mechanism to them. In this regard, Gallagher et.al. [10] provide a numerical characterization to help predict and understand the mechanism of bacterial

inactivation using DBD plasma. They use a simple exponential model using rate constants (chemical kinetics) and an ODE to solve for species concentration. Akishev et.al. [11] go one step further and use an emipirical mathematical approach to predict bacterial inactivation, taking into account not only inactivation of cells, but their reparation as well. Pintassilgo et.al. [12], [13], however, opened up a new venue of numerical modeling in plasma sterilization by using a kinetic model i.e. to solve for the different species concentration using a hydrodynamic model of equations. What is lacking is a connection between the kinetic and the exponential model- a model that can predict the kinetics of the plasma process using species chemistry modeling, while being able to connect the concentrations of the species as well as ionization rates predicted to the survival curve (that is obtained for that particular species).

This paper investigates ways in which the results of numerical modeling can be connected to those obtained in experiments. Solving this objective can be accomplished in a two-fold method- experimental and numerical. The numerical part of this objective can be achieved by running a set of numerical simulations modeling air chemistry in plasma, obtain the spatio-temporal profiles for electron, and ion density after a given time interval and consequently obtain the spatio-temporal rate of ionization. The experimental half of this solution would consist of running the devices inoculated with yeast, shown in Fig.(2) for required time intervals and obtaining time stamps on agar plates. The challenge would be to correlate the experimental and numerical results. This is further described in Section IV.

II. Experimental Procedure

Fig.2 (a) above shows a schematic of the device used to generate DBD plasma. Fig. 2(b) shows the actual device used. A 1mm thick FR4 sheet overlaid with tin-coated copper is etched as per the design shown in the schematic. The device measures 3.4x4 cm^2. The thick black lines represent copper electrodes 1.5 cm long and 0.2 cm wide. The thinner electrode connecting them is 0.5 cm wide. As can also be noticed from 2(b), around the electrodes, a darker square can also be seen. This represents the bottom square of tin-coated copper. This is also represented by the grey-colored area in 2(a). This square is grounded, while the top electrode is powered. Fig.2(c) shows the device when is being fired. Notice that the plasma is confined to only around the electrodes, while the rest of the grey area seems to be unaffected by the glow. This is an important point to consider, when analyzing the effect of afterglow on sterilization. This will be discussed later in Section III.

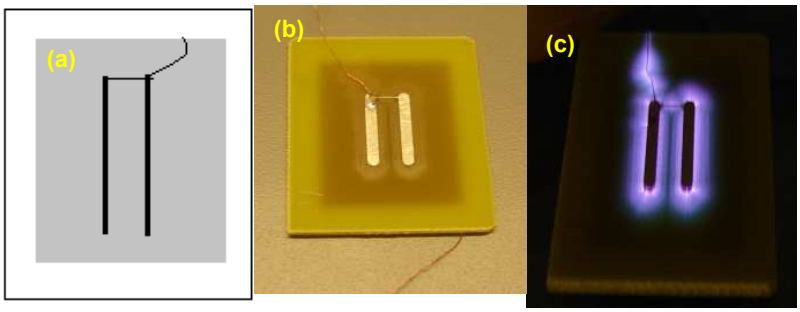

Fig.2(a) Schematic of the DBD device used (b) The DBD device not fired (c) The DBD device when fired

The experimental setup used has been described in a previous paper[16]. It consists of a function generator which generates a 14 kHz sinusoidal wave, which is amplified using an audio amplifier. This amplified signal is then sent to a HV transformer, which ramps up the signal to the order of kilovolts and is finally input into the device. The final signal powering the device has a peak-to-peak voltage of 12 kV and a power of about 7 W. 40 µl of S.cerevisiae (yeast) is then deposited onto the device and spread using an inoculating loop, such that it covers the entire grey area and allowed to dry. Once the device is run for the required time interval, plasma is switched off and the device is carefully stamped onto a SAB agar plate. Once it has rested on the agar plate for about 5 seconds, it is removed using a pair of disinfected forceps. Extreme care is taken to ensure that a) the device is not stamped too heavily onto the plate, causing a distortion of the yeast pattern b) removing the device with the forceps does not

disturb the yeast pattern stamped on the plate. These plates are then incubated at 37°C for 24-48 hours and examined afterwards. Owing to the qualitative nature of these tests, they have been replicated a number of times to ensure uniformity.

For the numerical simulation part of this paper, we refer to previous works by Roy et.al.[14] wherein the equations governing dynamics of electrons, ions and fluid are solved to obtain spatiotemporal distributions of electron, ion and neutral density as well as electric field. Further papers[15] present simulations with a real gas model with air-like N_2/O_2 mixture. Plasma is nothing more than a mixture of different ionized species, electrons and neutrals. It has been hypothesized by previous papers[11]-[12] that a determining factor in plasma sterilization could be the reaction of the different chemical species produced with the microorganism in question. A micro-organism in the simplest of senses is a chemical, albeit a complex one, comprised of carbon, hydrogen and oxygen atoms, as well as supplementary chemical atoms. Plasma consists of chemical species such as N_2^+, NO^- and oxidizing species O_2+, O^- and even O_4^+. Thus, when the above mentioned microorganism is introduced to such chemical species, a chemical reaction, similar to etching might take place, wherein some of the atoms comprising the micro-organism react with the plasma species. The objective of numerical simulation for such a process is to model these chemical reactions. A more elaborate explanation is provided in Section III.

III. Numerical Details

Two-dimensional two species plasma governing equations as well as Navier-Stokes equations are solved in this study. The unsteady transport for ions and electrons is derived from the first-principles in the form of conservation of species continuity. The species momentum flux is embedded in the momentum equations using the drift-diffusion approximation under isothermal conditions. Such an approximation can predict general characteristics of plasma discharges.[12] The continuity equations for concentration of positive ion n_i and electron n_e together with Poisson equation for electric field vector $\mathbf{E}$ (E_x, E_y):

$$\nabla \cdot (\varepsilon \mathbf{E}) = -e(n_e - n_i) \tag{1}$$

$$\begin{aligned} &\frac{\partial n_i}{\partial t} + \nabla \cdot \left(n_i \mathbf{V}_i \right) = \alpha \left| \Gamma_e \right| - r n_i n_e \\ &\frac{\partial n_e}{\partial t} + \nabla \cdot \left(n_e \mathbf{V}_e \right) = \alpha \left| \Gamma_e \right| - r n_i n_e \\ &\left| \Gamma_e \right| = \sqrt{(n_e V_e)_x^2 + (n_e V_e)_y^2} \end{aligned} \tag{2}$$

where n_e and n_i are number densities of electron and ion respectively, $\mathbf{V}$ (V_x, V_y) is the species hydrodynamic velocity, $r \sim 2\times10^{-7}$ cm^3/s is the electron-ion recombination rate, ε is the dielectric constant, the elementary charge e is 1.6022×10^{-19} C, and subscript i and e are positive ion and electron, respectively. The discharge is maintained using a Townsend ionization scheme. The ionization rate is expressed as a function of electron flux $\left|\Gamma_e\right|$ and Townsend coefficient α :

$$\alpha = Ap \exp\left(-B/(|\mathbf{E}|/p)\right) \tag{3}$$

where A and B are pre-exponential and exponential constants, respectively, p is the gas pressure, and E is the electric field. The ionic and electronic fluxes in equation (2) are written as:

$$\begin{aligned} n_i \mathbf{V}_i &= n_i \mu_i \mathbf{E} - D_i \nabla n_i \\ n_e \mathbf{V}_e &= -n_e \mu_e \mathbf{E} - D_e \nabla n_e \end{aligned} \tag{4}$$

The final form of the above equations is expressed below:

$$\frac{\partial n_i}{\partial t}+\frac{\partial}{\partial x}\left\{n_i\mu_i E_x - D_i\frac{\partial n_i}{\partial x}\right\}+\frac{\partial}{\partial y}\left\{n_i\mu_i E_y - D_i\frac{\partial n_i}{\partial y}\right\}=\alpha\left|\Gamma_e\right|-rn_in_e$$
$$\frac{\partial n_e}{\partial t}+\frac{\partial}{\partial x}\left\{-n_e\mu_e E_x - D_e\frac{\partial n_e}{\partial x}\right\}+\frac{\partial}{\partial y}\left\{-n_e\mu_e E_y - D_e\frac{\partial n_e}{\partial y}\right\}=\alpha\left|\Gamma_e\right|-rn_in_e \quad (5)$$

where $\mu_i = 1.45\times10^3 / p$ (cm^2/sV) is the ion mobility, $\mu_e = 4.4\times10^5 / p$ (cm^2/sV) is the electron mobility, D_i and D_e are the ion and electron diffusion coefficients calculated from the Einstein relation which is a function of ion and electron mobility as well as ion and electron temperature, i.e. $D_i = \mu_i T_i$ and $D_e = \mu_e T_e$. The electric field is given by $\mathbf{E} = -\nabla\varphi$, i.e., the gradient of electric potential φ. The system of equations (1) is normalized using the following normalization scheme: t/t_0, $z_i = x_i/d$, $N_e = n_e/n_0$, $N_i = n_i/n_0$, $u_e = V_e/V_B$, $u_i = V_i/V_B$, and $\phi = e\varphi/k_BT_e$ where k_B is Boltzmann's constant, $V_B = \sqrt{k_BT_e/m_i}$ is the Bohm velocity, reference length d which is usually a domain characteristic length in the geometry.

The numerical model for solving DBD plasma governing equations uses an efficient finite element algorithm for solving partial differential equations (PDE) approximately. The solution methodology anchored in the modular MIG flow code is based on the Galerkin Weak Statement (GWS) of the PDE which is derived from variational principles. An iterative sparse matrix solver called Generalized Minimal RESidual (GMRES) is utilized to solve the resultant stiff matrix. The fully implicit time stepping procedure along with the Newton-Raphson scheme is used for dealing with this nonlinear problem. The solution is assumed to have converged when the L_2 norms of all the normalized solution variables and residuals are below a chosen convergence criterion of 10^{-3}.

IV. Results & Discussion

4.1. Experimental Results

Given below are the results of the stamp tests. Each figure shows the image of a SAB plate, onto which a device, that has been run for a particular time interval has been stamped. Fig.3(a) represents the control device, which has not been run at all. Fig 3(b) represents a device that has been run for 60s and Fig.3(c) represents a device that has been run for 120s. Fig.3(d) is a schematic of the device, to serve as a visual interpretation of the yeast stamp that you see in the other three figures. This schematic has already been described in Fig.2(a). Note that the red rectangle, shown in Fig.3(d) represents the area over which plasma is seen. As can be inferred from Fig.2(c), the plasma is confined only to the area around the electrodes. Fig.3(a) clearly depicts a high concentration of yeast, wherein you can also see a slight imprint made by the two electrodes. For clarity, two orange lines mark where the copper electrodes exist on the device. One can observe that the yeast imprint on the control is heavily populated everywhere except the electrodes, which implies that maybe the transfer from the copper electrodes is more restricted than that from the FR4. In Fig.3(b), we see that there is a reduction in yeast concentration, especially in the gap between the electrodes. In Fig.3(c), we see that there is an almost complete reduction in yeast concentration at 120s. Yeast on the top of the electrodes remains unaffected, while the yeast between and around the electrodes seems to have been effectively inactivated.

Comparing Figs. 3(b) and 3(c) with 3(a), a couple of points can be noted.

a) Yeast inactivation seems to be spreading in an annular pattern around the electrodes, as depicted equivalently by the red square in Fig.3(d).At 60s, yeast outside the area covered by the electrodes remains unaffected, while at 120s, the yeast outside this area also seems to be inactivated effectively.
b) The yeast on top of the electrodes does not seem to be affected a great deal by the plasma, suggesting that the rate of ionization on top of the electrodes is less than that in between the electrodes.
c) There is a heavy concentration of yeast along the edge of the inoculated square in 3(b), while 3(c) shows a reduced concentration along the edges. For an electrode of such a small surface area, the effect of direct plasma is far less significant than the effect of the afterglow given off by such a plasma. In the afterglow of a plasma, the electric field is absent but chemical species generated due to the plasma de-excite and

participate in secondary chemical reactions, which etches the micro-organisms further and increases the rate of chemical inactivation

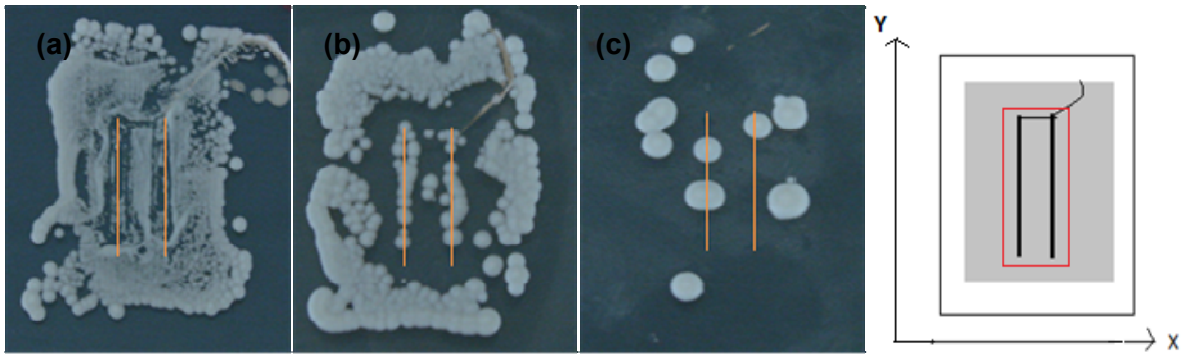

Fig. 3(a) Control stamp (b) Stamp at 60s (c) Stamp at 120s (d) Schematic of the device.

The annular pattern in which the killing spreads outwards, as time progresses, can be empirically measured by using a non-dimensional parameter S(t). If we define **r(t) as inner killing radius** such that it is equivalent to drawing a circle of radius r, bordering the red rectangle shown in Fig.3(d). During a stamp test, yeast is spread on the grey rectangle containing the electrodes (as shown in Fig.3(d)). When the device is stamped, it shows a rectangular pattern corresponding to this. **R is defined as the outer radius**, such that it is equivalent to drawing a circle of radius R, bordering the grey rectangle, representing the total stamp, as shown in Fig.4, wherein the two white lines represent the electrode imprints. Both r and R are determined by matching the circular cross-sectional area with the respective rectangular cross-sectional area. S is the ratio of r over R. As time progresses towards the complete sterilization time of 2 min (for yeast), it is expected that r increases outwards and hence S →1.

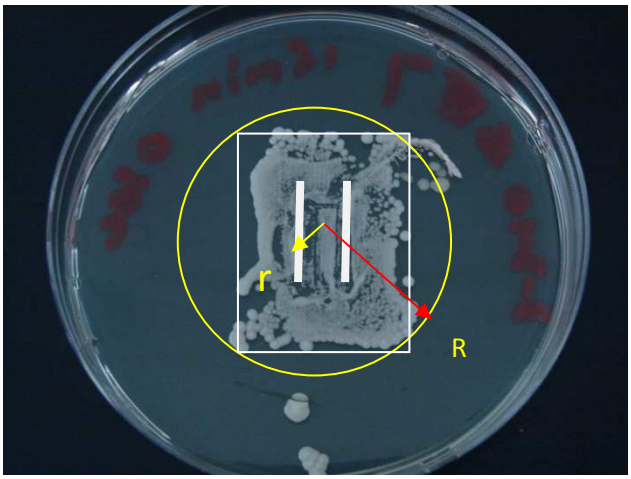

Fig.4. A stamped plate at t=0s.

A more detailed discussion about the effect of ionization on S(t) follows in Section 4.3.

4.2. Numerical Simulation

As highlighted in Section II, the objective of numerical simulation is to model the chemical reactions that might occur between a bacterial micro-organism and the chemical species present in plasma. Consider a micro-organism like yeast, or as it is known by its micro-biological moniker, S.cerevisiae. Its macro-molecular constituents are proteins, glycoproteins, polysaccharides, polyphosphates, lipids and nucleic acids. The yeast cell itself is

surrounded by a rigid cell wall, comprised of glycoproteins and polysaccharides. Polysaccharides have a general formula of $C_x(H_2O)_y$, where x is usually a large number between 200 and 2500. The repeating units in the polymer backbone are often six-carbon monosaccharides and hence the general formula can also be represented as $(C_6H_{10}O_5)_n$, wherein $40 \leq n \leq 3000$. These hydrocarbon chains undergo chemical reactions wherein they are oxidized by oxidizing species or hydrolysed by hydroxyl like species. Each of these chemical reactions has a corresponding reaction rate constant that determines how fast or slow the reaction takes place. The rate of a reaction determines the concentration of chemical species produced. Hence for a chemical reaction wherein, a polysaccharide reacts with a chemical species produced in plasma, the corresponding increase in concentrations of new species formed and decrease in concentration of the polysaccharide can be simulated using reaction rate constants and chemical rate equations. As a first step towards that process, a RF plasma, 2-species model comprising of ions and electrons, driven by a frequency (υ)= 14 kHz and voltage V= 12000 V p-p is simulated for the geometry as shown in Fig.2(a). As described in Section III, the Poisson Equation and continuity equations for the ion and electron species (relevant to air chemistry) are numerically solved to obtain the spatiotemporal variation of electron, ion and neutral density.

Accordingly, consider the ionization plot shown below, which depicts the spatial variation of the average rate of ionization (per m^3s). The average rate of ionization has been calculated using the values of ionization (varying spatially) obtained over each 0.5π phase of one whole cycle of time period 2π. As can be observed in Fig. 5, the rate of ionization seems to peak at x= 1.3 & 1.5 cm as well as 1.9 & 2.1 cm. Elsewhere the rate of ionization is fairly low. The length between x=1.3 and 1.5 as well as x=1.9 and 2.1, which represents the two electrodes, also shows fairly low rates of ionization. This implies that the rates of ionization are highest around the edge of the electrodes, while on the electrodes as well as elsewhere on the device, the rate of ionization is lower. This coincides with the results obtained from the stamp test, wherein we see initial yeast inactivation around the electrodes and only later, do we see inactivation elsewhere on the device.

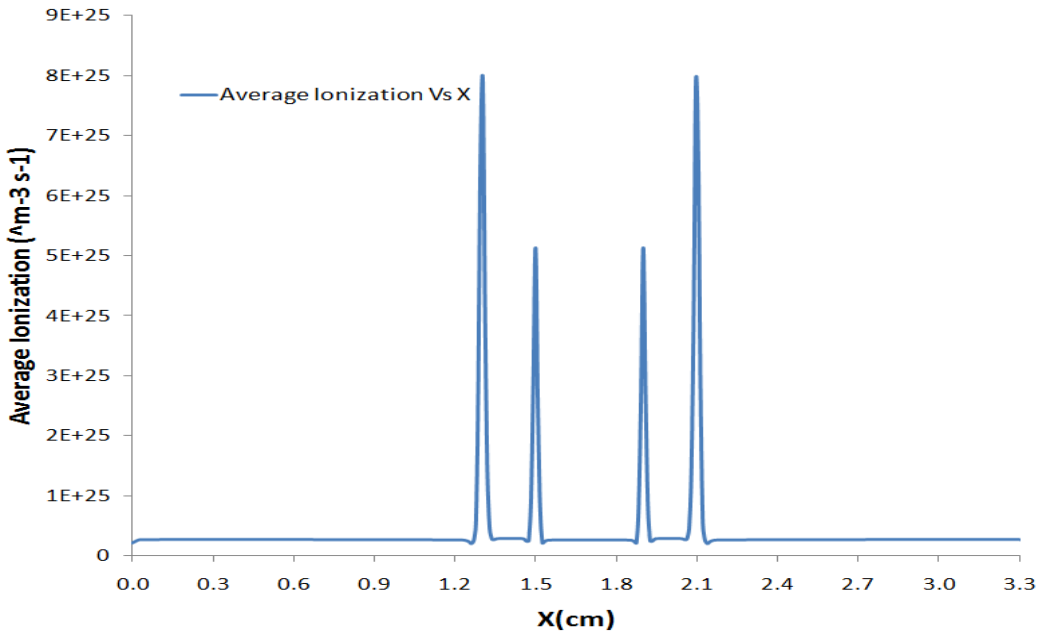

Fig. 5. Plot of Rate of Ionization (I) along the X –axis of the given device

4.3. Correlating the experimental & numerical results.

From preliminary results of numerical modeling as well as experimental stamp tests, it is clear that there exists a correlation between rate of ionization and rate of killing. Fig.(6) depicts the plot of 1-S versus time (s). As can be approximated from the curve fit, the trend seems to closely resemble an exponential trend.

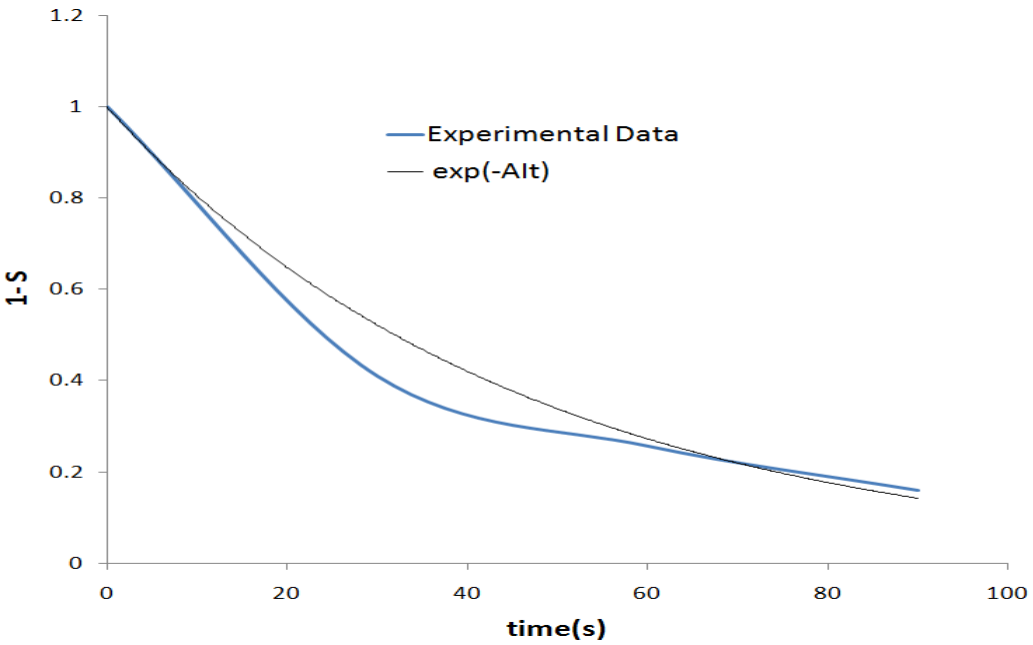

Fig.6. Plot of 1-S versus time for S.cerevisiae (yeast)

An exponential curve has been fitted to represent the trend of the curve. This exponential curve is of the form

$$S = 1 - e^{-AIt} \tag{6}$$

Wherein A is a normalization constant, I is the average rate of ionization and t is the time in seconds.
Here AI= 0.022, as evaluated from the curve fit. A is a normalization constant. Noting that the average rate of ionization, as obtained from Fig.5, is of the order of 4.25e+24, A is obtained to be equal to 5.17e-27 m^3.

The exponential relation shown herein is not absolute. The ionization rate plotted plotted has been obtained as a spatial average of the values over each 0.5 π phase of the cycle. Plotting ionization rate for the entire sterilization interval of 120s (for yeast) would be a phenomenal task in terms of simulation time. This particular simulation has been plotted only for two species. In order to accurately capture the chemistry in plasma sterilization, as described in Section II, a more complex model consisting of numerous other chemical species as well as the micro-organism has to be constructed. This model would have numerous coupled chemical reactions, all happening at the same instant, thus adding to computational complexity and time. Hence in order to reduce computational time, the numerical simulation has been allowed to run until a constant rate of ionization at each spatial location is reached. Thus this steady state value of ionization has been assumed to be the rate of ionization during the entire sterilization interval. Also, the ionization rate is definitely dependent on other plasma parameters such as driving voltage, driving frequency, biological species being tested, electrode geometry etc. There is a huge dependency on biological species being tested because different species take different times for complete inactivation to be achieved. However this is estimated by the factor 't' in (1). For the other parameters, we propose the following functional form for I = fn(ϕ, υ, *g*) where ϕ is the applied potential at a frequency *υ* and *g* denotes electrode geometric configuration. The preliminary value of I, in (1) has been obtained for a constant ϕ, υ and g. Further work needs to be done in order to understand the functional relationship between I and the parameters above. Sterilization tests have to be conducted for different driving voltages and different driving frequencies, S has to be plotted from the experimental data obtained from these sterilization tests and the same correlation has to be obtained in order to obtain an improved value for 'A'.

It is also to be noted that plasma sterilization is not a process wherein chemical reactions between the micro-organism and plasma species is the only killing mechanism . Other factors such as UV and heat also come into play, thus making simulating the plasma sterilization a highly complex process, involving coupled processes. However as a first step, simulating the air chemistry seems to serve as a reliable empirical predictor.

V.Conclusion

A preliminary study on a possible diagnostic tool that can be used to predict the rate of killing due to plasma sterilization, based on the rate of ionization due to plasma processes has been presented. The ionization rate (I) has been obtained by solving the governing equations for a 2-species RF plasma model. Experiments were conducted wherein a given concentration of yeast was exposed to 14 kHz, 12 kV DBD plasma over a time interval of 120s. Stamp tests at different time intervals show an exponentially increasing rate of sterilization. This has been expressed in terms of a non-dimensional parameter S. A preliminary exponential correlation has been obtained between S(t) and I. Future work needs to explore the dependence of I on various other plasma parameters such as frequency, voltage and the like. This empirical correlation would then help predict survival curves for other micro-organisms as well as give a better understanding of the physics of plasma sterilization.

VI. Acknowledgement

This work has been supported by grants from the Florida Board of Governors and SESTAR, Inc. The authors would also like to thank Dr.Jianli Dai, Emerging Pathogens Institute, UF for his invaluable help during the experimental phase of the project.

References:

[1] Cooper,M., 2009. Elucidation of Levels of Bacterial Viability Post- Non-Equilibrium Dielectric Barrier Discharge Plasma Treatment.

[2] Roth, JR., 1995. Industrial Plasma Engineering

[3] Kogelschatz,U., 2002. Dielectric-barrier Discharges: Their History, Discharge Physics and Industrial Applications. *Chemistry and Plasma Processing, Vol.23, No.1, March 2003*

[4] Montie,T.C., Wintenberg,K.K., Roth,J.R., An overview of research using the one atmosphere uniform glow discharge plasma (OAUGDP) for sterilization of surfaces and materials. *IEEE Trans. Plasma Sci. 28(2000) 41-50*

[5] Moisan,M., Barbeau,J., Moreau,S., Pelletier,J.,\ Tabrizian,M., Yahia,L'H., 2001. Low-temperature sterilization using gas plasmas: a review of the experiments and an analysis of the inactivation mechanism. *Intl. Journal of Pharmaceutics. 226, 1-21*

[6] Choi,Jai Hyuk., Han, Inho., Baik,Hong Koo., Lee,Mi Hee., Han,Dong-Wook., Park,Jong-Chul., Lee,In-Seob., Song,Kie Moon., Lim,Yong Sik. Analysis of Sterilization effect by pulsed dielectric barrier discharge. *Journal of Electrostatics 64(2006)17-22*

[7] Tanino,M., Xilu,W., Takashima,K., Katsura,S., Mizuno,A. Sterilization using Dielectric Barrier Discharge at Atmospheric Pressure. *Intl. Journal of Plasma Environmental Science & Technology, Vol.1, No.1*

[8] Deng,S., Cheng,C., Ni,G., Meng,Y., Chen,H., 2008. Bacterial Inactivation by Atmospheric Pressure Dielectric Barrier Discharge Plasma Jet. *Japanese Journal of Applied Physics, Vol.47, Issue 8, pp.7009*

[9] Fridman,A., 2008. Plasma Chemistry

[10] Gallagher,M., Vaze,N., Gangoli,S., Victor,N., et.al. *IEEE transcations on Plasma Science,Vol.35, #5, October 2007*

[11] Akishev,Y., Grushin,M., Karalnik,V., et.al., Atmospheric Pressure Nonthermal Plasma sterilization of microrganisms in liquids and on surfaces, Pure Appl. Chemistry, 2008

[12] Pintassilgo,C D., Loureiro,J., Guerra,V., Modelling of a N2-O2 flowing afterglow for plasma sterilization. *J.Phys.D.Appl.Phys.38(2005)417-430*

[13] Kutasi,K., Pintassilgo,C D., Coelho,P J., Loureiro,J., *Modelling of a post-disharge reactor used for plasma sterilization J.Phus.D:Appl.Phys.39 3978 (2006)*

[14] Singh K.P. and S. Roy, 2007. Modeling plasma actuators with air chemistry for effective flow control, Journal of Applied Physics, 101 (12) 123308

[15] K. P. Singh, S. Roy, and D. Gaitonde, Fluid Dynamics and Flow Control Conference, San Francisco, CA, June 2006 _AIAA, Washington, D.C., 2002_, Paper No. AIAA-2006-3381; S. Roy, K. P. Singh, and D. Gaitonde, 45th AIAA Aerospace Sciences Meeting and Exhibit, Reno, NV, 2007 AIAA, Washington, D.C., 2002_, Paper No. AIAA-2007–0184.

[16] N. Mastanaiah, U. Saxena, J. Johnson, and S. Roy, 2010, Inactivation of Yeast cells using Dielectric Barrier Discharge, AIAA-2010-1340, 48th AIAA Aerospace Sciences Meeting, Orlando, FL.